Resilient Structures and Sustainable Construction
Edited by Pellicer, E., Adam, J. M., Yepes, V., Singh, A., and Yazdani, S.

ISBN: 978-0-9960437-4-8

DEFORMATION AND ULTIMATE STRENGTH OF R/C ARCH UNDER ASYMMETRIC LOAD

TAKASHI HARA

Dept of Civil Engineering and Architecture, National Institute of Technology, Tokuyama College, Shunan, Japan

In this paper, the structural behavior of R/C arch was investigated by use of the finite element method considering combined geometric and material nonlinearities. Also, the experimental analyses were conducted based on the numerical results. The deep and shallow arches were adopted as the model. The arches were pin supported at both ends and were subjected to asymmetric concentrate loads in vertical direction. The deformation and the load bearing characteristics were investigated from the load-deflection behavior and the crack propagation patterns. From both numerical and experimental analyses, the load bearing behavior and the ultimate strength of R/C arches were in good agreement.

Keywords: Numerical analysis, Experimental work, Crack, Crush, Snap buckling, Structural characteristics.

1 INTRODUCTION

Arches are popular structural elements. They resist against the external forces and show large load bearing capacity due to transfer external forces into inner force. They have been applied to the bridge structure and the architectural elements with elegant shapes. Also, arches change to vaults when arches are copied to the transverse direction. Domes are formed when arches are copied around the vertical axis passing the arch crown. The structural behavior of arch is important to assess the shell behavior. For the guideline of the design of the reinforced concrete (R/C) shell structure, only IASS recommendation of reinforced concrete shell (IASS 1976) and ACI 318 (ACI 2011) were established. The strength of R/C arch can analogize R/C shell strength.

In this paper, prior to R/C shell structural analysis, R/C arch was analyzed numerically and experimentally. In the previous study (Kirita *et al.* 2013), the loading was applied to the full span of arch. However, in this analysis, R/C shell arches were tested under asymmetric loading condition. Also, the structural behavior of R/C arch was investigated by use of the finite element method considering combined geometric and material nonlinearities. From both experimental and numerical analyses, the structural behavior of R/C shell was presented.

2 EXPERIMENTAL WORK

2.1 Specimens

Specimens were made by using the steel mold under machine processing to prevent the initial imperfection of R/C arch and to make smooth placing of concrete. Moreover, two kinds of the rises were adopted. One was a shallow arch (Sarch) whose rise is 200 mm, the other was a deep

arch (Darch) whose rise is 500 mm. The dimensions of the specimen were indicated in Table.1 and Figure 1. The span B, width H and thickness t are the same. However, the opening angle θ and the radius r are different. Three main rebars of the diameter φ = 3.05 mm are arranged on the top and the bottom, and spacers were used to hold 10 mm concrete cover (Figure 1). Spiral reinforcement was arranged around the supports to reinforce them to prevent the crushes.

Table 1. Dimensions of R/C arch.

Symbol	Sarch	Darch
B	2000mm	2000mm
H	80mm	80mm
h	200mm	500mm
R	2600mm	1250mm
t	40mm	40mm
θ	45.24°	106.26°
h/B	1/10	1/4

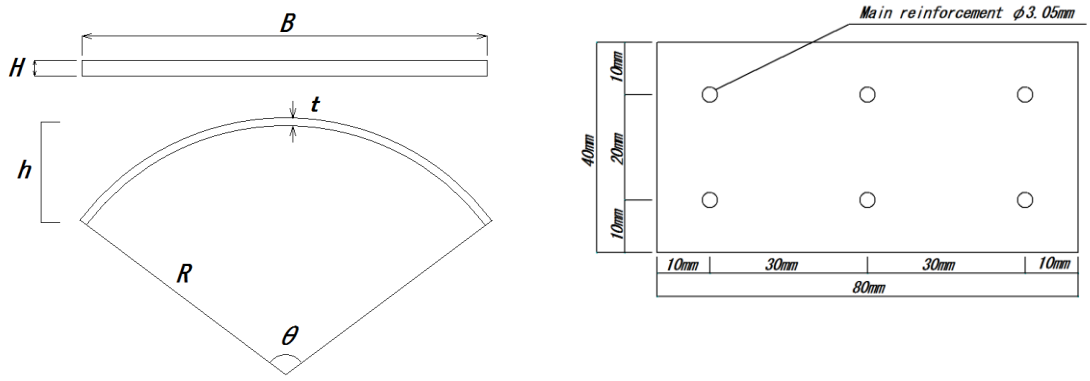

(a)Plan and Elevation. (b)Cross section.

Figure 1. Dimensions of R/C arch.

2.2 Loading Conditions

Loading apparatus was composed of the steel frame, the hydraulic jacks and the supports. The length was 3000mm. The outline of the apparatus is shown in Figure 2. Supports were arranged on the foundation H-steel. Each support was a pin support to fix a steel ball of φ 20mm on M16 socket bolt at both ends.

At any loading conditions, loading points are changed for Sarch and Darch. Steel columns were placed at the point of a jack and loading head was applied according to the curved surface of the arch, to apply the load vertically. The steel plate was inserted from both top and bottom of arch surfaces at the location of a jack to prevent the sliding of loading head.

Loading test was performed using the hydraulic pressure system manual jack. Loading position was set to 1 point which divided the length of the half of the arch into two equal length. Three points and five points shows the loading position divided into four and six equal length, respectively (see Figure 3(a)). The loading direction was vertical. The loading position was the center of the arch width at the loading point. Loading was applied gradually, by a hydraulic pressure jack up to the failure. At each loading stage displacements were measured.

Displacements were measured up to failure at a surface of an arch from one to five in Figure 3(b). The load was measured using the load transducer during the loading test.

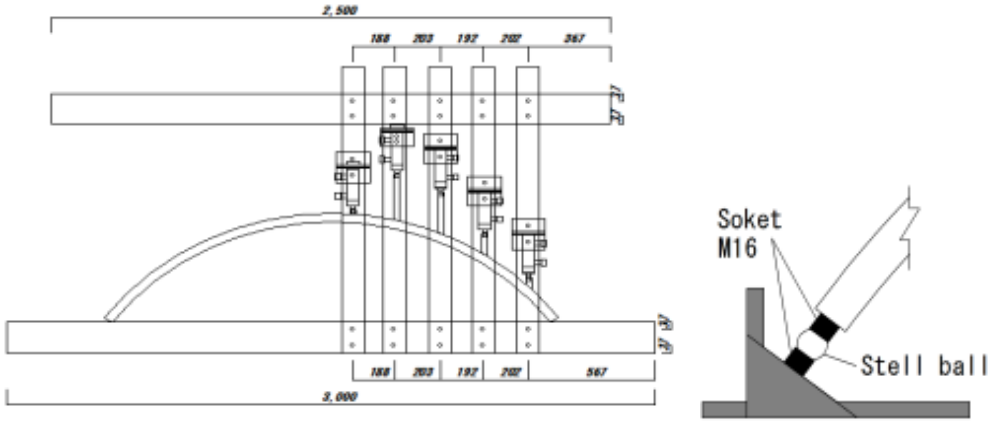

Figure 2. Loading apparatus.

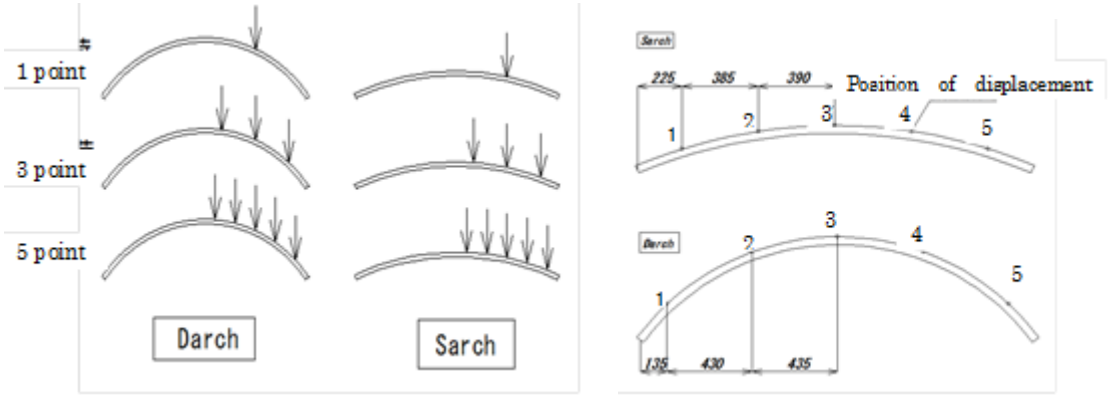

(a) Loading Position. (b) Position of displacement transducer.

Figure 3. Loading conditions and measuring position.

2.3 Experimental Results

Figure 4(a) and Figure 4(b) indicate the relation between the load displacement obtained from experiment under five-point loading for Sarch and Darch, respectively (Tsuyama and Hara 2016). Abscissa shows displacements. Positive displacements are in downward. Ordinate indicates the total applied load. Both specimens show the same deformation pattern. Displacements under loading points four and five indicate positive displacement (downward) independent of the height of the rise, and the other side (points one and two) indicates negative displacement (upward). The center of the arch shows small displacement in downward.

Load-deformation curve of Sarch indicates steeper comparing with Darch. In case of Sarch, at load 5kN, the displacement glows suddenly without load increment. This phenomenon is a snap thorough. Therefore, Sarch shows brittle failure. However, the Darch does not show such brittle failure. Darch was failed by flexure. Figure 5 shows that the cracks concentrate below the

loading point under one point loading on Sarch. In case of five points loading, the cracks on Sarch occur in the wider area than that under one point loading. In case of Darch, the same results are obtained.

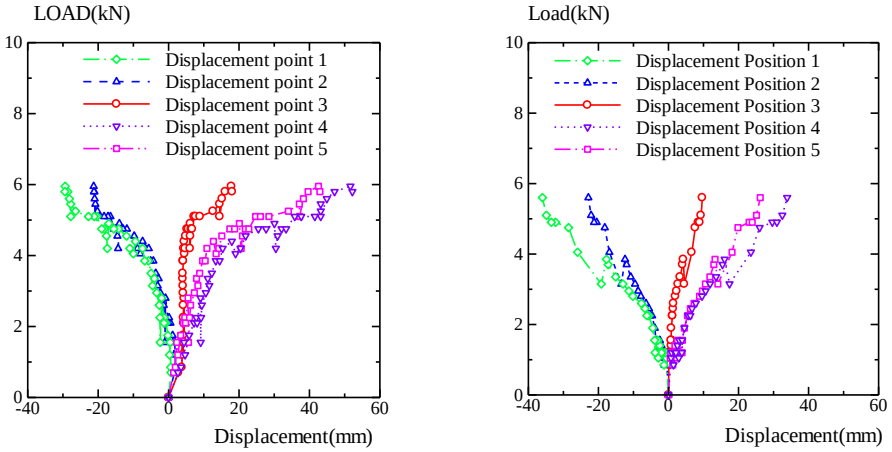

(a) Sarch. (b) Darch.

Figure 4. Load displacement relation.

Figure 5. Deformation and cracks on Sarch under one point loading.

3 NUMERICAL ANALYSIS

3.1 Numerical Model

The structural behavior of R/C arch was investigated by use of the finite element method considering combined geometric and material nonlinearities. Figure 6 shows the numerical models. In numerical analysis, full model of R/C arch was analyzed. R/C model was divided into isoparametric solid elements with 20 nodes. Table 2 shows the material properties of the concrete and steels.

The inelastic behavior of concrete possesses the recoverable strain components and irrecoverable strain components. Under tri-axial stress state, the yield function depends not only on the mean normal stress but also on the second deviatoric stress invariant (Hinton 1988). The yield condition of tri-axial compressive concrete is expressed by Drucker-Prager criterion (Hinton 1988, Hara 2004). Parameters adopted in the criterion are defined by the Kupfur's experiment (Kupfer and Hilsdorf 1969). It is assumed that the initial yield begins when the equivalent stress exceeds $0.3f_c$ (f_c: compressive strength of concrete). Also, the crushing condition of concrete is described as a strain control phenomenon and the crushing condition is defined as like as the yield function (Hinton 1988, Hara 2004). The response of concrete in tension is modeled as a linear-elastic brittle material and maximum tensile stress criteria are employed. After cracking, to

evaluate the stiffening of reinforced concrete, the stress reduction of the concrete normal to the cracked plane is assumed as an exponential degradation curve (Hara 2004, Hinton 1988).

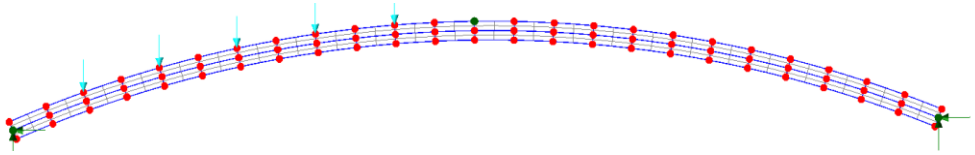

Figure 6. Numerical model.

Table 2. Material properties.

Concrete		Steel	
Young's modulus (GPa)	24.1	Young's modulus (GPa)	217
Compressive Strength(MPa)	36.3	Hardening parameter	0.01
Tensile Strength(MPa)	3.63	Tensile strength (MPa)	342

3.2 Numerical Results

Figure 7 (a) and Figure 7 (b) indicate the relation between the load displacement obtained from numerical analysis under five-point loading for Sarch and Darch, respectively. Both numerical results are 15% larger than experimental one (see Figure 4). However, a snap buckling is detected and the cracks and the deformation are represented well (see Figure 8). In Figure 8, the rectangle and the cross denote a crack and a crush in concrete.

Figure 9 shows the relation between the ultimate strength of R/C shell and the number of loading points obtained from experimental results. The more the loading points are, the larger the ultimate strength is. The phenomena are strong under full loading conditions.

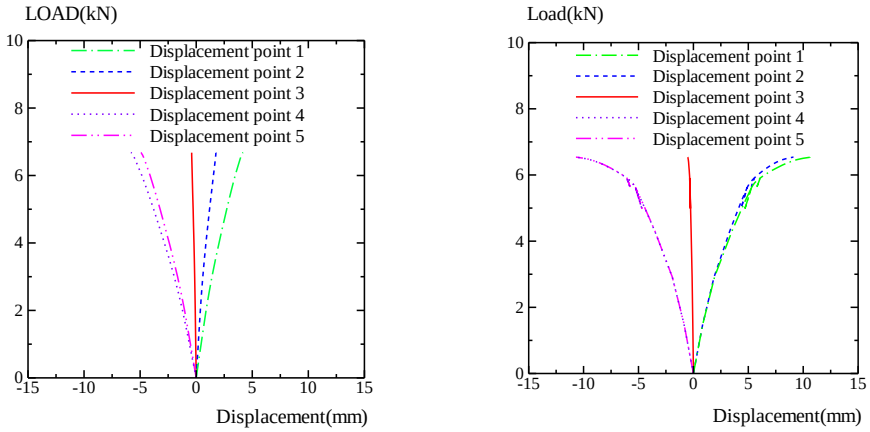

(a) Sarch. (b) Darch.

Figure 7. Load displacement relation by numerical analysis.

Figure 8. Deformation and cracks on Sarch under one point loading.

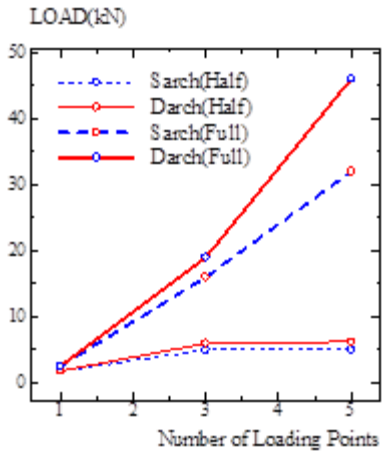

Figure 9. Ultimate strength of R/C arch with the number of loading points (experiment).

4 CONCLUSIONS

In this paper, numerical and experimental analyses of R/C arch were investigated under an asymmetric loading. From both analyses, the following conclusions are obtained: (i) The ultimate strength of both shallow and deep arches reached almost the same under asymmetric loading. The deep arch was predominately failed by flexure but the shallow arch was failed by the snap through; (ii) The more the loading points, the larger the ultimate strength; and (iii) The arch at full load shows the larger ultimate strength than that under asymmetric loading.

Acknowledgements

This research work was done under the supports of Grants-in-Aid for Scientific Research, Japan Ministry of Education, Culture, Sports, Science and Technology (No. 26420573).

References

American Concrete Institute (ACI), *Building Code Requirements for Structural Concrete (ACI 318-11) and Commentary (2011) Chapter19*, p.315-321, 2011.

Hara, T., Dynamic Analysis of R/C Cooling Yower Shells Under Earthquake Loading, *5th International Symposium on Natural-Draught Cooling Towers*, 283-291, 2004

Hinton, E., Numerical Methods and Software for Dynamic Analysis of Plates and Shells, Pineridge Press Swansea U.K, 1988.

IASS Working Group NR5, *Recommendations for Reinforced Concrete Shells and Folded Plates*, pp.11-57, IASS, 1979.

Kirita, T., Mitsunaga, H., and Hara, T., Load Carrying Capacity of Reinforced Concrete Arch Structure Considering Loading Condition, *Advanced Materials Research*, Vol. 831, pp. 105-109, Dec. 2013

Kupfer, H. and Hilsdorf, K. H., Behavior of Concrete Under Biaxial Stress, *ACI Journal*, 66, 656-666, 1969.

Tsuyama, T. and Hara, T., *Load Carrying Capacity of an Arch Subjected to the Load in One Half*, 3rd SCESCM, P-6, September 2016.